



## **Optimization of tubelength in TiO<sub>2</sub> nanotube – a computational approach**

**S.HarshaVarthan<sup>1</sup>, V. Saravanakannan<sup>2</sup>, R. Chandiramouli<sup>2</sup>**

<sup>1</sup>School of Mechanical Engineering, SASTRA University, Tirumalaisamudram, Thanjavur -613 401, India

<sup>1</sup>School of Electrical & Electronics Engineering, SASTRA University, Tirumalaisamudram, Thanjavur -613 401, India

**Abstract:** In the present work, TiO<sub>2</sub> nanotube length is optimized using artificial neural network. The length of TiO<sub>2</sub> nanotube can be varied with the parameters such as applied voltage and anodization time in anodization of Ti foil method. Various range of tube length from 0.400 -10.998 $\mu$ m can be grown when voltage is kept at 10V and the anodization time is adjusted from 1 - 45 hours. The tube length of 0.400-11 $\mu$ m can be synthesized, when the voltage is kept at 20 V and the anodization time is adjusted from 1 -70 hours. The computed results of the tube length are found to be in close agreement with the experimental results with an error of 0.00403. The optimization process of TiO<sub>2</sub> nanotube length reduces the strain and effort of researchers while synthesizing TiO<sub>2</sub> nanotubes.

**Keywords:** titanium oxide; nanotube; anodization; tubelength.

### **1. Introduction**

Transition metal oxides (TMO) are mainly used as chemical sensors, catalyst and in solar cells. One among the transition metal oxides is titanium oxide (TiO<sub>2</sub>). TiO<sub>2</sub> exhibits three polymorphism namely, rutile, anatase and brookite phase. TiO<sub>2</sub> naturally occurs as a rutile in some acid igneous rocks and metamorphic rocks and is also in sedimentary rocks & beach sands. The metastable anatase and brookite phases convert irreversibly to the equilibrium rutile phase upon heating above temperatures in the range 600°-800°C. TiO<sub>2</sub> have tremendous applications in various fields such as in photo catalytic applications [1], gas sensing [2], photo electrolysis [3], polymer based bulk heterogeneous photovoltaics [4], energy storage devices such as Li – ion batteries and super capacitor [5]. 1-D nanowire and nanotube of TiO<sub>2</sub> with high surface to volume ratio possess significant useful and unique properties. Moreover, the morphology of TiO<sub>2</sub> nanostructures gives rise to numerous applications. TiO<sub>2</sub> can be synthesized by many methods such as sol gel transcription process using organo gelato templates [6], pulsed laser deposition [7], hydrothermal techniques [8] and anodization of titanium in fluid based electrolyte leads to controlled dimension of nanotube synthesis [9]. The thickness of TiO<sub>2</sub> nanostructures plays an important role in deciding different properties such as physical, chemical, electrical and mechanical properties. Meiling et al synthesized TiO<sub>2</sub> nanotubes by anodic oxidation and electro deposition methods [10]. Pei et al prepared TiO<sub>2</sub> nanotubes by a hydrothermal method [11]. Tang et al synthesized TiO<sub>2</sub> nanotubes by anodization of Ti films at room temperature [12]. Yuren et al reported the synthesis of TiO<sub>2</sub> nanotubes using a hybrid synthetic strategy [13]. Cui synthesized TiO<sub>2</sub> nanotubes by facile microwave-assisted hydrothermal method [14].

The artificial neural network (ANN) find its applications in time series prediction [15], fitness approximation [16], robotics [17], control including computer numerical control [18], generation of

conductivity map on the ground [19], reliability analysis of steel structures [20] and thermal analysis of heat exchangers [21]. The motivation behind the present work is to fine-tune the nanotube dimension of TiO<sub>2</sub> using the artificial neural network and to optimize the nanotube length during. From the literature survey, it is known that not much work is done to optimize TiO<sub>2</sub> nanotube dimension using ANN. In the present work, the nanotube anodization of Ti sheets length of TiO<sub>2</sub> is optimized using ANN and the results are reported.

## 2. Computational details

The success of the artificial neural network depends on their architecture, learning algorithm, which is used in the transfer function and the number of neurons. In this present work, back propagation algorithm (BPA) neural network is used to estimate the length of TiO<sub>2</sub>. A simple architecture of neural network is shown in Figure 1, which has two input neurons in the input layer, three neurons in the hidden layer and two neurons in the output layer. Usually BPA is a supervised learning algorithm, which reduces over all systems to minimum and it uses the sigmoid activation function  $f(x)=1/1+e^{-x}$ . Usually during the learning or training process, an interconnection between the input, hidden and output layers are established. This interconnection between the layers enables the signal transfer between the layers. The intensity of the signals can be determined with the help of the weights of the corresponding signals. This can be done by iteratively changing the weights of the corresponding signals between the neurons and the sum of the squared errors between the calculated weights and expected weights can be minimized by the model selected.

During the learning process, the initial weight vectors  $W_0$  are updated using the following equation,

$$W_i(k+1)=W_i(k)+\mu(T_i-O_i)f'(W_i x_i)x_i$$

where  $W_i$  is the weight matrix associated with  $i^{\text{th}}$  neuron,  $x_i$  is the input of  $i^{\text{th}}$  neuron,  $O_i$  is the actual output of the  $i^{\text{th}}$  neuron,  $T_i$  is the target output of the  $i^{\text{th}}$  neuron and  $\mu$  is the learning rate parameter.

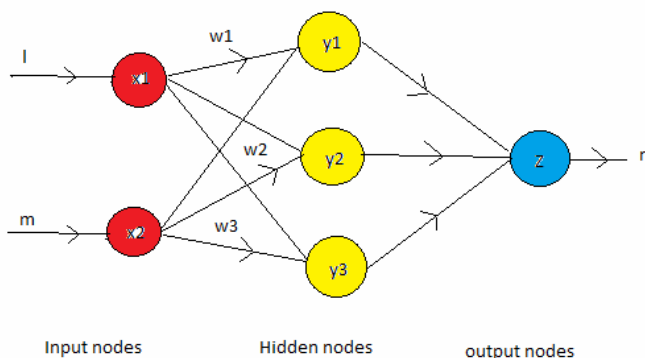


**Fig. 1 Basic Neural Network Model**

In the present work, the data obtained from the experiments [22] are given as input. The modelled network consists of two input nodes with voltage between the electrodes and the anodization time as inputs. Finally the result of the tube length is obtained when the voltage between the electrodes and the anodization time is given as input. For the number of training cycles being  $1.82 \times 10^9$ , the mean error obtained is 0.000403. The cycle learning rate is 0.6000 with the momentum of 0.8000. After the running cycles for several time with voltage being 10, 20 and 25 V, wide range of tube length are calculated.

## 3. Results and discussion

Usually in anodization of Ti foils, titanium anode and a platinum cathode is immersed in an aqueous electrolyte of dilute acid to which a small dc voltage is applied. The surface layer is sufficiently resistive to prevent current flow. Electrolyte composition also primarily decides whether the oxide film is porous or it forms a barrier. Initially, pits are formed on the TiO<sub>2</sub> layer, then pores start growing to form the ordered

nanotube arrays in the substrate. On anodization, the pore growth takes place, after certain time dissolution occurs along the inter pore region, finally ordered nanotube arrays are formed. It is observed that TiO<sub>2</sub> nanotube structure is grown on increasing the voltage beyond 23V and by adding 0.5% hydrofluoric acid electrolyte in a ratio of 1:7, mechanically stronger nanotubes can be synthesized. Fig. 2 represents the anodization process of Ti foils to form TiO<sub>2</sub> nanotubes. The input data are given from the reported work and the optimization of TiO<sub>2</sub> nanotube are calculated using ANN [22]. Finally querying rows has been added for testimony of the artificial neural network and the errors are minimized as stated above and the data are verified.

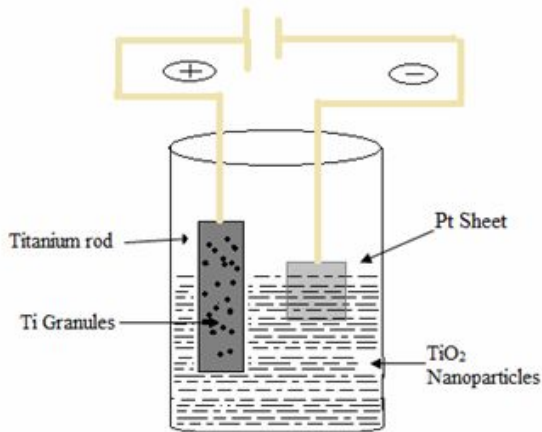


Fig. 2 Anodization of Ti foils to form TiO<sub>2</sub> nanotubes

**Training process**

The result obtained from the experiment [22] is used in the growing the network. The voltage and anodization time are given as the input in the two input nodes and the tube length is obtained as output. Fig. 3 illustrates the reported TiO<sub>2</sub> nanotubes synthesized at different voltage for various time duration.

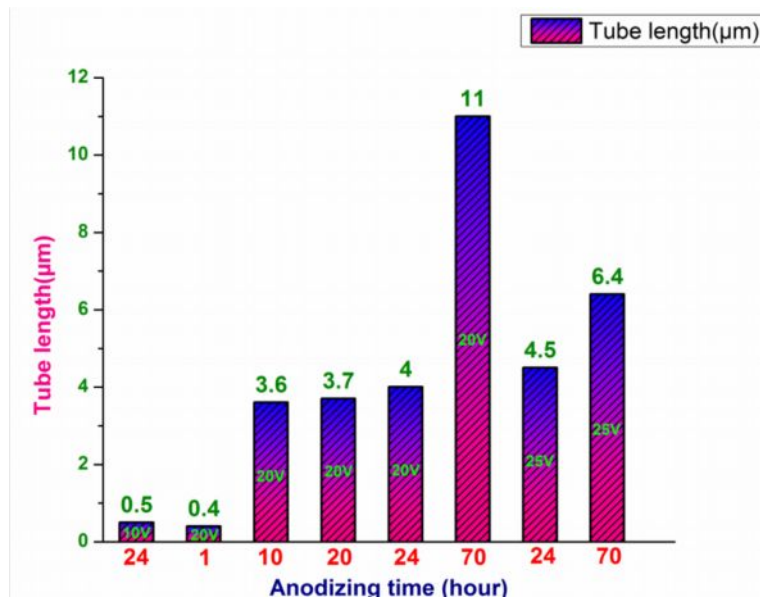


Fig. 3 Reported TiO<sub>2</sub> nanotubes synthesized at different voltage -ref [22]

**Testing process**

After training the back propagation neural network with the data obtained from the anodization experiment, test rows are generated, then the correctness of the neural network is tested by giving input and the training ANN once again. The results obtained have error of 0.000403 and the correctness of the results are validated as in Fig. 4.

O:0	I:1	I:2	O:0	I:1	I:2	O:0	I:1	I:2
4.3559	25.0000	65.0000	4.0900	25.0000	25.0000	3.7889	10.0000	31.0000
4.5023	25.0000	66.0000	4.0900	25.0000	26.0000	5.9411	10.0000	34.0000
4.6037	25.0000	66.5000	4.0901	25.0000	29.0000	9.7262	10.0000	37.0000
4.7299	25.0000	67.0000	4.0901	25.0000	31.0000	10.9633	10.0000	40.0000
4.8871	25.0000	67.5000	4.0901	25.0000	33.0000	0.4022	10.0000	22.0000
5.0825	25.0000	68.0000	4.0902	25.0000	46.0000	0.4202	10.0000	23.0000
5.3244	25.0000	68.5000	4.0901	25.0000	35.5000	1.1004	10.0000	26.0000
5.6224	25.0000	69.0000	4.0902	25.0000	47.0000	2.7433	10.0000	29.0000
5.9859	25.0000	69.5000	4.0903	25.0000	49.0000	0.5003	10.0000	24.0000
0.8421	20.0000	3.0000	3.9994	25.0000	4.0000	0.4000	10.0000	1.0000
2.2909	20.0000	6.0000	4.0910	25.0000	52.0000	2.7433	10.0000	29.0000
3.3596	20.0000	9.0000	4.0915	25.0000	53.0000	0.5000	10.0000	24.0000
3.8201	20.0000	12.0000	4.0923	25.0000	54.0000	0.4000	20.0000	1.0000
3.9929	20.0000	15.0000	4.0935	25.0000	55.0000	2.7433	10.0000	29.0000
4.0554	20.0000	18.0000	4.0953	25.0000	56.0000	0.5000	10.0000	24.0000
4.0777	20.0000	21.0000	4.0982	25.0000	57.0000	0.4000	20.0000	1.0000
4.0885	20.0000	27.0000	4.1026	25.0000	58.0000	3.6000	20.0000	10.0000
4.0895	20.0000	30.0000	4.1094	25.0000	59.0000	3.7000	20.0000	20.0000
4.0899	20.0000	33.0000	4.1200	25.0000	60.0000	4.0000	20.0000	24.0000
4.0902	20.0000	36.0000	4.1363	25.0000	61.0000	11.0000	20.0000	70.0000
4.0906	20.0000	39.0000	4.1616	25.0000	62.0000			
4.0922	20.0000	42.0000	4.2008	25.0000	63.0000			
4.0980	20.0000	45.0000	4.2616	25.0000	64.0000			
4.1193	20.0000	48.0000	4.3559	25.0000	65.0000			
4.1985	20.0000	51.0000	4.5023	25.0000	66.0000			
4.4936	20.0000	54.0000	4.6037	25.0000	66.5000			
5.5907	20.0000	57.0000	4.7299	25.0000	67.0000			
8.7324	20.0000	60.0000	4.8871	25.0000	67.5000			
10.8766	20.0000	63.0000	5.0825	25.0000	68.0000			

Fig. 4 Training data set given for the neural network

### Optimization of TiO<sub>2</sub> tube length

Thirty three data have been generated by keeping 10V as input voltage and varying anodization time, thirty four data have been generated keeping 20V as input voltage and varying anodization time, thirty three data have been generated keeping 25V as input voltage and varying anodization time. Fig. 5 represents the growth process of TiO<sub>2</sub> nanotubes. Various range of tube length from 0.400 -10.998 $\mu$ m is observed when voltage is kept at 10V and the anodization time is adjusted from 1-45 hours. The tube length of 0.400-11 $\mu$ m can be grown, when the voltage is kept at 20 V and the anodization time is adjusted from 1 -70 hours. When the voltage is kept at 25 V, 4.5 -6.4  $\mu$ m can be synthesized. From the results, it is inferred that for anodization time of 24-70 hours, tube length of 4.500 -6.400  $\mu$ m can be synthesized. Fig. 6 illustrates the optimized growth prediction of TiO<sub>2</sub> nanotube length for various voltages. Moreover, the higher conductivity of electrolyte is the influencing factor for the growth of TiO<sub>2</sub> nanotubes. Initially, the growth of TiO<sub>2</sub> nanotube increases. However, for the time period of 10 hours to 20 hours, the chemical etching leads to improved conductivity of electrolyte [22]. Meanwhile, the top debris results in the breakage of nanotube length, which gives rise to decrease in the tube length for higher voltages as shown in the Fig. 6. The importance of the present work is a wide range of results can be generated, which is hard to obtain experimentally and is also time consuming process.

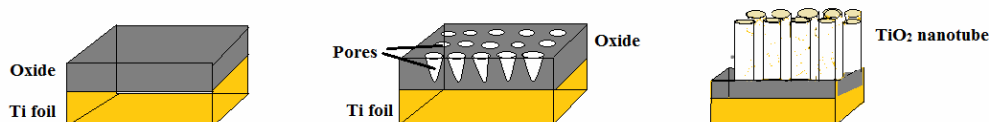
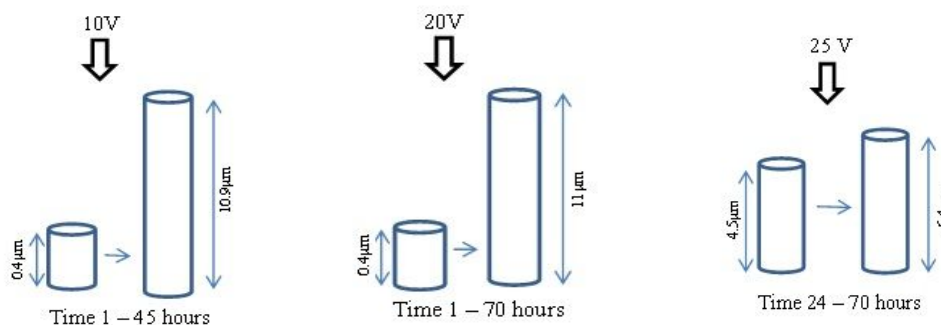


Fig. 5. Growth process of TiO<sub>2</sub> nanotubes

From the above results it is clear that by varying the voltage and anodization time TiO<sub>2</sub> nanotubes of different lengths ranging from 0.4 to 11  $\mu$ m can be obtained and the parameter for different length can be

obtained using ANN. Although many methods of diagnosis have been reported, the preparation of TiO<sub>2</sub>nanotubes by anodization in electrolytic solution have proven to be one of the efficient method. Furthermore, incorporating the experimental results with the artificial neural network gives the accurate and optimized result. Besides, the work proves that it is legitimate to use artificial neural network in obtaining the results.



**Fig. 6. Optimized growth prediction of TiO<sub>2</sub> nanotube length for various voltages**

## 5. Conclusion

In summary, the tube length of TiO<sub>2</sub> nanotubes is optimized using ANN. Even though there are number of experimental procedures to synthesis TiO<sub>2</sub> nanotube of various sizes, researchers still find it difficult to adjust the parameters to obtain the desired length of TiO<sub>2</sub> nanotube. Moreover, ANN is a reliable method to optimize TiO<sub>2</sub> nanotube tubelength by feeding the experimental data and generating the tubelength without going for the tedious experimental methods. In the present work, an attempt has been made to optimize the tube length of TiO<sub>2</sub> nanotubes. The desired tubelength of TiO<sub>2</sub> nanotubes can be obtained byanodization method using this approach. It also reduces the strain and effort of the researchers for obtaining the correct parameters to get the desired TiO<sub>2</sub> nanotube length.

## References

1. Dai J, Yang J, Wang X, Zhang L and Li Y, Enhanced visible-light photocatalytic activity for selective oxidation of amines into imines over TiO<sub>2</sub>(B)/anatase mixed-phase nanowires, *Appl. Surf. Sci.*, 2015, 349, 343–352.
2. Yan W, Hu M, Wang D, and Li C, Room temperature gas sensing properties of porous silicon/V<sub>2</sub>O<sub>5</sub>nanorods composite, *Appl. Surf. Sci.*, 2015, 346, 216–222.
3. So H and Pisano A. P, Micromachined passive phase-change cooler for thermal management of chip-level electronics, *Int. J. Heat Mass Transf.*, 2015, 89, 1164–1171.
4. Donets S, Pershin A and Baeurle S. A, Computation of full polymer-based photovoltaic nanodevices using a parametrized field-based multiscale solar-cell approach, *Org. Electron.*, 2015, 22, 216–228.
5. Shimizu T and Underwood C, Super-capacitor energy storage for micro-satellites: Feasibility and potential mission applications, *Acta Astronaut.*, 2013, 85, 138–154.
6. Yan J, Liu J, Lei H, Kang Y, Zhao C and Fang Y, Ferrocene-containing Thixotropic Molecular Gels: Creation and A Novel Strategy for Water Purification, *J. Colloid Interface Sci.*, 2015, 448, 374–379.
7. Nematollahi M, Yang X, Gibson U. J and Reenaas T. W, Pulsed laser ablation and deposition of ZnS : Cr, *Thin Solid Films.*, 2015, 590, 28–32.
8. Pei Z, Pei J, Chen H, Gao L and Zhou S, Hydrothermal synthesis of large sized Cr<sub>2</sub>O<sub>3</sub> polyhedrons under free surfactant, *Mater. Lett.*, 2015, 159, 357–361.
9. Cummings F. R, Muller T. F.G, Malgas G. F and Arendse C. G, Investigation of the growth and local stoichiometric point group symmetry of titania nanotubes during potentiostatic anodization of titanium in phosphate electrolytes, *J. Phys. Chem. Solids.*, 2015, 85, 278–286.

10. Zhong M, Zhang G and Yang X, Preparation of Ti mesh supported WO<sub>3</sub>/TiO<sub>2</sub> nanotubes composite and its application for photocatalytic degradation under visible light, *Mater. Lett.*, 2015, 145, 216–218.
11. Liu P, Liu H, Liu G, Yao K and Lv W, Preparation of TiO<sub>2</sub> nanotubes coated on polyurethane and study of their photocatalytic activity, *Appl. Surf. Sci.*, 2012, 258, 9593–9598.
12. Tang Y, Tao J, Zhang Y, Wu T, Tao H and Zhu Y, Preparation of TiO<sub>2</sub> nanotube on glass by anodization of Ti films at room temperature, *Trans. Nonferrous Met. Soc. China.*, 2008, 19, 192–198.
13. Li Y, Yan Y, Su Q, Xie E and Lan W, Preparation of Graphene – TiO<sub>2</sub> nanotubes / nanofibers composites as an enhanced visible light photocatalyst using a hybrid synthetic strategy, *Mater. Sci. Semicond. Process.*, 2014, 27, 695–701.
14. Cui L, Hui K. N, Hui K.S, Lee S. K, Zhou W, Wan Z. P and Chi-Nhan Ha Thuc., Facile microwave-assisted hydrothermal synthesis of TiO<sub>2</sub> nanotubes, *Mater. Lett.*, 2012, 75, 175–178.
15. Prema V and Uma Rao K, Development of statistical time series models for solar power prediction, *Renew. Energy.*, 2015, 83, 100–109.
16. Davarynejad M, Ahn C. W, Vrancken J, Van Den Berg J and Coello C. A. C, Evolutionary hidden information detection by granulation-based fitness approximation, *Appl. Soft Comput. J.*, 2010, 10, 719–729.
17. Vongbunyong S, Kara S and Pagnucco M, Learning and revision in cognitive robotics disassembly automation, *Robot. Comput. Integr. Manuf.*, 2015, 34, 79–94.
18. Zhao D, Ni W, Zhu Q, A framework of neural networks based consensus control for multiple robotic manipulators, *Neurocomputing.*, 2014, 140, 8–18.
19. Kalogirou S. A, Florides G. A, Pouloupatis P. D, Christodoulides P and Joseph-stylianou J, Artificial neural networks for the generation of a conductivity map of the ground, *Renew. Energy.*, 2015, 77, 400–407.
20. Kala Z, Sensitivity and reliability analyses of lateral-torsional buckling resistance of steel beams, *Arch. Civ. Mech. Eng.*, 2015, doi: 10.1016/j.acme.2015.03.007.
21. Sekhar B. S, Lototskyy M, Kolesnikov A, Moropeng M. L, Tarasov B. P and Pollet B.G, Performance analysis of cylindrical metal hydride beds with various heat exchange options, *J. Alloys Compd.*, 2015, 645, S89–S95.
22. Yoriya S and Bao N, TiO<sub>2</sub> Nanotube Array Films Grown in DMSO / EtOH-Based Electrolyte : Anodization Current Response and Solvation Effect, *Int. J. Electrochem. Sci.*, 2014, 9, 7182–7197.

\*\*\*\*\*